Journal of Electroanalytical Chemistry xxx (2010) xxx–xxx

Contents lists available at ScienceDirect

Journal of Electroanalytical Chemistry

journal homepage: www.elsevier.com/locate/jelechem

# An efficient method for fabrication of disk-shaped scanning electrochemical microscopy probes with small glass-sheath thicknesses

Horacio L. Bonazza, José L. Fernández *

*Programa de Electroquímica Aplicada e Ingeniería Electroquímica (PRELINE), Facultad de Ingeniería Química, Universidad Nacional del Litoral, Santiago del Estero 2829, (S3000AOM) Santa Fe (Santa Fe), Argentina*

ARTICLE INFO

*Article history:*
Received 28 June 2010
Received in revised form 19 August 2010
Accepted 2 September 2010
Available online xxxx

*Keywords:*
SECM probes
Disk microelectrodes
Approach curves
Platinum tips

ABSTRACT

This work describes a method for fabrication of disk microelectrodes for scanning electrochemical microscopy (SECM) tips. A sharpened platinum wire is sealed into a borosilicate glass capillary and is thermally projected out of the capillary as a tip. The disk microelectrode is obtained by mechanical polishing of the protruding glass-shrouded wire apex. What make this method distinctive are the following details: (1) The Pt-containing capillary is embedded into a polymer support to carry out a secure polishing of the tip apex; once the disk is exposed, the polymer is dissolved. (2) Disk exposure is revealed by an electrical detection method. (3) As no manual sharpening of the glass tip is required, very small glass-sheath thicknesses can be obtained ($R_g$ = sheath radius/microelectrode radius < 3). The fabrication of tips with radii larger than 0.3 μm is relatively straightforward (success rate near 90%) with this method. SECM approach curves (positive and negative feedback), SEM and optical microscopy were used to characterize the described tips.



## 1. Introduction

The successful application of any of the scanning probe microscopy techniques relies on the quality of the utilized probe, and the scanning electrochemical microscopy (SECM) is not an exception. The SECM probe (or tip) is a sharpened microelectrode of any geometry [1]. The overall probe dimension (including the insulating material) is small enough that the approaching to a surface (substrate) at a distance smaller than the microelectrode dimension is possible. The lesser is the amount of insulating material around the microelectrode, the higher is the probability to attain smaller tip-substrate distances. Even though nowadays SECM employs tips with microelectrodes of any geometry, the classical feedback mode is benefited from using inlaid microelectrodes such as disks. On this sense, by using disk-shaped microelectrode tips the positive feedback (or thin-layer-cell) current for a certain tip-substrate distance is maximized and the sensitivity of the technique is optimized.

Available methods for fabrication of SECM probes have been reviewed several times during the last decade [2–6]. The most employed method for fabrication of disk-shaped SECM tips is the classical heat-sealing of a cylindrical metal wire into a glass capillary, followed by polishing of the cross section to expose the glass-embedded disk [3]. Mechanical manual sharpening of the lateral walls of the capillary using an abrasive pad (sandpaper, lapping film) is carried out until a thin thickness of the glass sheath is obtained. This procedure is simple and straightforward as long as the disk diameter is larger than typically 5 μm. In these conditions, and depending on the patience and ability of the operator, the ratio between the glass-sheath radius and the microelectrode radius ($R_g$) can be readily decreased down to near 2 with little risk. These tips are robust and work very well in many environments. For preparation of tips with disk diameters below 5 μm by this classical method, some complications arise [3]. Metal wires with these diameters are hard to manipulate, and generally come covered by a silver layer (which is removed before sealing) to improve handling. Besides, for these microelectrode dimensions it is quite difficult to arrive to $R_g$ values smaller than 10 by a manual polishing of the glass-sheath lateral walls. In spite of these complications, this still is a very useful method for fabrication of disk-shaped tips with diameters down to 1 μm, although an operator with extraordinary patience is required. So far the most popular method to fabricate disk-shaped tips with diameters below the micrometer is based on the use of a laser-based pipette puller [7,8]. A metal wire is inserted in the center of a borosilicate or quartz glass capillary, which is locally heated using a laser source and simultaneously pulled in several pre-programmed steps. During these steps the metal and the glass are melted and drawn out together until they are cut in two pieces that contain the conical wire sealed into the sharpened capillary. A very careful final polishing and sharpening is required to finally expose the metal disk. Due to the extreme fragility of the

* Corresponding author. Tel.: +54 342 4571164x2519.
*E-mail address:* jlfernan@fiq.unl.edu.ar (J.L. Fernández).

1572-6657/$ - see front matter © 2010 Elsevier B.V. All rights reserved.
doi:10.1016/j.jelechem.2010.09.004

glass-sealed microelectrode apex, this last polishing step is generally performed under the exhaustive observation of the tip approach to the polishing pad, for example by using a micropipet beveller and a video monitor. Although this method has been applied for fabrication of tips in many reported studies [9–14], its success rate depends very much on the training and skills of the operator [3]. Other methods that rely on sealing a conical fiber and polishing of the tip apex by means other than mechanical, such as ultra-high-frequency electrochemical etching [15] and Field-Ion-Beam (FIB) milling [16] have been recently reported.

In this context, it is clear that an alternative methodology for fabrication of disk-shaped microelectrode tips that stands mainly on its simplicity and high success rate could be highly appreciated by SECM users. On this sense, the present work explains a procedure for preparation of SECM tips with low $R_g$ values, which is essentially based on the first procedure described by Bard and co-workers [17]. Some key modifications were included trying to make the procedure more efficient (high percentage of successful tips) and to avoid steps that could be too sensitive to the operator skills.

## 2. Experimental

### 2.1. Chemicals and materials

Borosilicate glass capillaries (o.d. = 1.5 mm, i.d. = 1.0 mm) were from Paralwall (Argentina). Platinum microelectrodes were fabricated using platinum wires (diameter = 25 μm, hard) from Alfa Aesar (Ward Hill, MA). Silver epoxy EpoTek E4110 (Epoxy Technology, Billerica, MA) was used to make electrical contacts. Self-cure acrylic for dental repairs from Subiton Laboratories (Argentina) was used to support the tips during polishing. Chloroform (Anedra, Argentina), acetone (Cicarelli, Argentina), ferrocenemethanol (Aldrich, St. Louis, MO), calcium chloride (Merck, Germany), sodium sulfate (Merck), and hydrochloric acid (Merck), were used as received. Piranha solution had 70 vol.% sulfuric acid (Merck) and 30 vol.% hydrogen peroxide (Cicarelli). Water used in all experiments was first deionized with an exchange resin, then doubly distilled, and finally treated with a Purelab purifier (Elga Labwater, resistivity $\geqslant$18.2 MΩ cm).

### 2.2. Instrumentation

The tips were monitored at the different preparation steps using an optical microscope Nikon model Optiphot furnished with filters for contrast enhancement, a 10× eyepiece and objectives of up to 100× (maximum total magnification = 1000×). A camera Nikon model FX-35DX was used to acquire micrographs. A graduated scale (Nikon) was used to generate distance scales in the micrographs. For SEM analysis, the tips were coated with a sputtered gold film and observed using a microscope JEOL model JSM-35C. Sputtering of gold was carried out using a sputter coater SPI 12157-AX operating under an Ar atmosphere at 18 mA. A home-built SECM instrument, consisting of a bipotentiostat and a micro-positioning system, was used for electrochemical evaluation of tips (approach curves and cyclic voltammetry). The bipotentiostat was a PG 340 (Heka Elektronik, Germany) with an ITC-16 board. Tip position was controlled with a Nanocube P-611.3S closed-loop XYZ nano-positioning system (Physik Instrumente, Germany) with a maximum travel length of 100 μm per axis, which was driven by an E-664 voltage amplifier/servo controller (Physik Instrumente). Both the bipotentiostat and the positioning system were commanded via the software PotMaster (Heka Elektronik).

### 2.3. Fabrication of Pt tips

#### 2.3.1. Etching of Pt wires

A piece of approximately 1 cm of a 25-μm-diameter Pt wire was attached to a copper wire (0.5 mm diameter) using silver epoxy and cured at 80 °C for 3 h. The Pt-wire end was placed concentric to a Pt ring counter-electrode (3 mm inner diameter) and immersed about 2 mm into a 4.5 M $CaCl_2$–1 M HCl solution. An ac (50 Hz) voltage of 3 V was applied between the Pt wire and the ring counter-electrode using a variable ac transformer. Gas evolution and Pt dissolution occurred for about 5 s until the immersed part of the Pt wire completely dissolved. The bottom end of the Pt wire that remained outside the solution (attached to the copper wire) resulted with a sharp conical shape. The wire was carefully rinsed by immersion in water and finally dried in air.

#### 2.3.2. Sealing of Pt wires into borosilicate glass capillaries

Borosilicate glass capillaries were cleaned using piranha solution for 10 min, rinsed with water, and dried in an oven at 100 °C. A clean sharpened Pt wire was inserted into a clean capillary leaving the cone at about 3 mm from the capillary end. The Pt cone was sealed into the capillary by heating and melting the capillary end with a Bunsen flame, and taking especial care to get the wire and the capillary centered. No vacuum was necessary as long as the capillary and wire were perfectly clean. The sealed wire was repetitively heated to a glowing condition during intervals of 2 s until the arrival of the Pt apex to the glass surface was visually

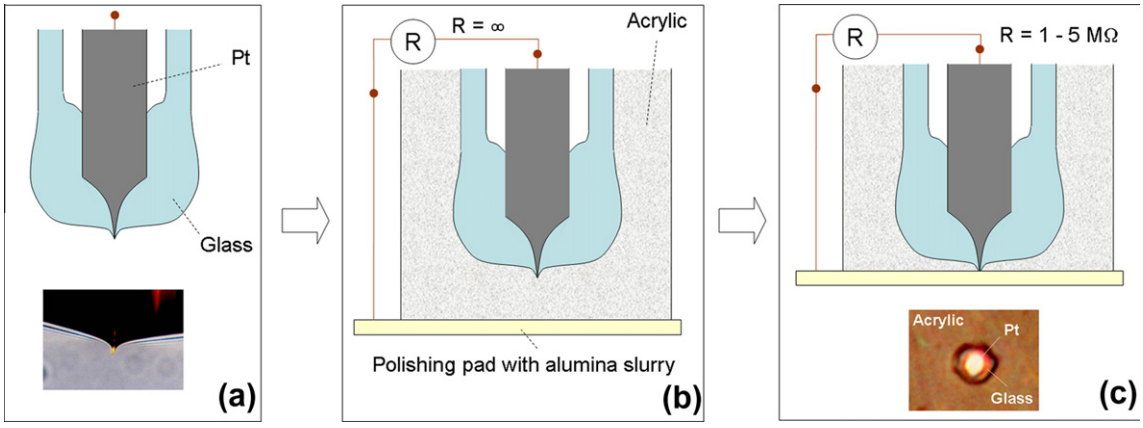


**Fig. 1.** Scheme of the procedure for polishing Type-A tips. The optical micrographs show the lateral view of a sealed and protruding sharpened Pt wire (a) and the upper view of a polished tip secured in acrylic (c).

Please cite this article in press as: H.L. Bonazza, J.L. Fernández, J. Electroanal. Chem. (2010), doi:10.1016/j.jelechem.2010.09.004

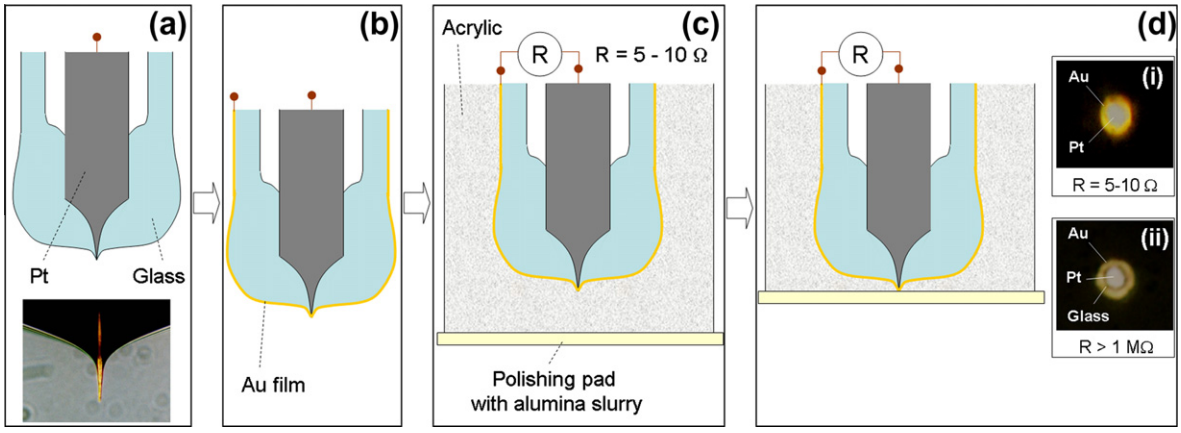


**Fig. 2.** Scheme of the procedure for polishing Type-B tips. The optical micrographs show the lateral view of a protruding sharpened Pt wire exposed at the apex (a) and the upper views of a polished tip secured in acrylic before (d-i) and after (d-ii) the glass-sheath ring was complete.

evident. At this stage, a protruding cone was clearly visible under a magnifier lens and two different situations could occur, which are schematized in Figs. 1 and 2, respectively. In Type-A capillaries, the Pt wire was completely sealed in glass (e.g. that shown in Fig. 1a), while in Type-B capillaries the very end of the Pt cone was exposed (e.g. that shown in Fig. 2a). Cyclic voltammetry in solution of ferrocenemethanol (FcMeOH) was used to determine whether the cone was exposed or not. Well-defined steady-state voltammograms were obtained on Type-B electrodes while no current was detected on Type-A tips upon scanning the Pt potential.

*2.3.3. Coating of the Type-B capillary walls with a metal layer*

The outside walls of the Type-B capillaries were coated with a gold film deposited by sputtering for 100 s. A 0.2-mm-diameter copper wire was connected to the upper side of the gold coating using silver paint (Fig. 2b).

*2.3.4. Securing the capillary into an acrylic slab*

Each capillary was supported from its upper side standing as vertical as possible, and was introduced into a cylindrical Teflon mold (o.d. = 7.2 mm, i.d. = 5 mm, length ≅ 1.5 cm). Self-cure liquid acrylic was prepared by mixing the solid polymer and the liquid monomer using a mass-to-volume ratio of 1 g $cm^{-3}$. As soon as both components were thoroughly mixed, the self-cure acrylic was poured into the Teflon mold and let to cure for 24 h. After this curing time, the Teflon container was removed. As a result, a cylindrical slab of acrylic embedding the capillary was obtained (Figs. 1b and 2c).

*2.3.5. Polishing of the bottom section and stopping at an early exposition of the disk*

The bottom section of the cylindrical acrylic piece was sanded using coarse sandpaper until the sealed capillary was at less than 2 mm from the surface. From this point, polishing was continued with a sequence of finer sandpapers (until 2500 grit). A final polishing step with aqueous slurry of alumina 0.3 μm was applied until the end of the capillary was a few microns below the surface. For a Type-A capillary, an ohmmeter (0.2 GΩ maximum reading) was connected between the copper wire attached to the Pt wire and a wire immersed in an aqueous dispersion of 0.3-μm alumina. Polishing was gently continued while monitoring the resistance reading, which was out of scale while the capillary was completely embedded in acrylic (Fig. 1b). As soon as the polishing reached the capillary apex and the disk was exposed, the detected resistance showed intermittent changes. If polishing was continued, the registered resistance dropped to values in the order of the MΩ (Fig. 1c). On the other hand, for a Type-B capillary an ohmmeter was connected between the sealed Pt wire and the external gold film. Polishing with a dispersion of 0.3-μm alumina in water was gently continued while the resistance reading was permanently monitored. A small (5–10 Ω) resistance was measured due to electrical contact between the Pt wire and the Au film at the glass-free Pt apex (Fig. 2c). Once the polishing reached the Pt apex, a disk surrounded by a gold ring was exposed (Fig. 2d-i) and the detected resistance showed no changes. Upon continuing polishing the glass sheath also arrived to the surface. When the glass completely separated the disk from the ring (Fig. 2d-ii), the measured resistance showed a rapid increase to values in the order of MΩ, and the polishing was stopped.

*2.3.6. Removing the acrylic slab and metal coating*

The acrylic slab was dissolved in pure chloroform for 12 h. The capillaries with the polished tips were successively rinsed by immersion in clean chloroform, acetone and water, and dried in air with a heat gun. Finally, for Type-B capillaries, the gold layer was removed by chemical etching in $HNO_3$–HCl solution, and the copper wire plus the silver paint remaining at the top side were detached mechanically.

## 3. Results and discussion

### *3.1. Advantages of the described procedure*

In all tip-fabrication methods known so far, each involved step has a certain efficiency (or success rate) that is caused by factors that are beyond the control of the operator. In most methods for construction of disk-shaped tips, the steps that contain the highest risk, and consequently the lowest success rates, are the mechanical polishing and sharpening. Thus, special attention must be paid on these steps when trying to design a more efficient method. The presented procedure is based on a modification of the earliest method for fabrication of disk-shaped glass-sealed SECM tips proposed by Bard and co-workers [17]. This initial procedure had the great advantage that polishing was performed on a robust structure and no mechanical sharpening was required. Besides, low $R_g$ values were obtained. In spite of these advantages, the method was not widely applied and other procedures were preferred. This probably occurred due to the difficulties for obtaining the disk perfectly surrounded by a flat and leveled glass sheath by the proposed heating method. On this context, we designed a procedure

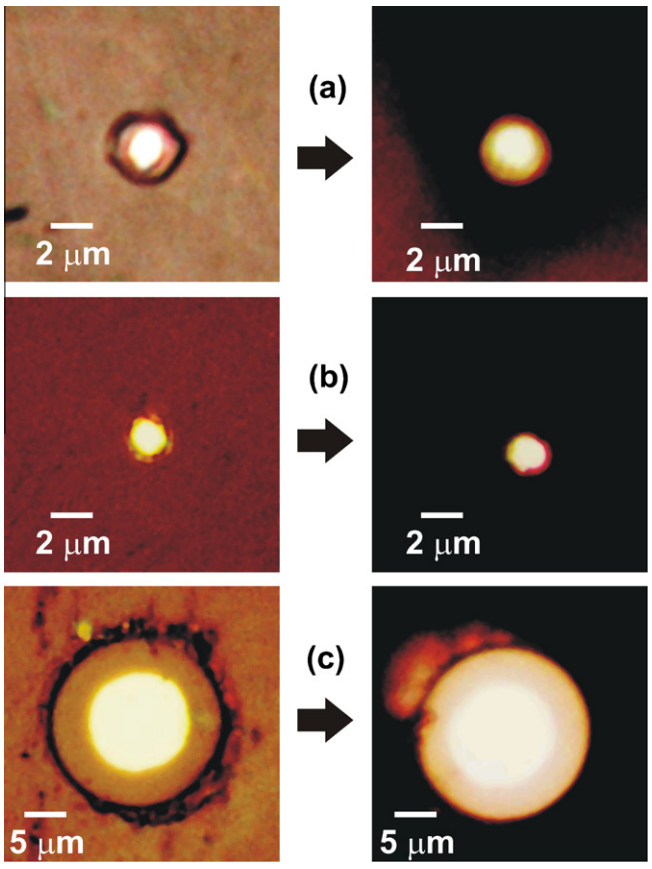


**Fig. 3.** Optical micrographs of upper views of polished tips before (left) and after (right) acrylic removal: (a) is a Type-A tip, while (b) and (c) are Type-B tips.

that keeps the advantages of the original procedure regarding to safe polishing and unnecessary sharpening, but adds control for defining a precise flat inlaid-disk shape.

Most of the steps of the method described in this work are based on well-known procedures that were already applied for fabrication of microelectrodes and SECM tips with other geometries. Thus for example, electrochemical sharpening of Pt wires is a common practice for construction of SECM conical and hemispheroidal tips [17–21] and STM probes [22,23]. Heat-sealing of Pt in glass is also a known procedure [3,17,21]. Moreover, polishing using an electrical method for detection of the disk exposure has successfully been used for fabrication of nanoelectrodes and nanopores [24]. However, supporting of the tip into a robust structure for a safe polishing during construction of SECM tips was surprisingly never explored, as it certainly was done for fabrication of regular nanoelectrodes [25]. On this sense, using acrylic as support is a very good option since this polymer is hard enough to protect the glass tip, and it is easy to apply and remove (by dissolving it in chloroform). Notwithstanding, due to the hardness differences, polishing of the acrylic-glass composite should still be performed with special care, very gently and avoiding excessive force against the polishing pad.

### 3.2. Characterization of tips

After polishing of the acrylic-secured capillaries, very flat and well-defined disk tips with flat glass sheaths at the same level of the Pt disks are obtained, as can be seen in the micrographs in Figs. 3 and 4. The micrographs in Fig. 3 show the upper views of three polished tips with different sizes and $R_g$ values before (left) and after (right) acrylic removal. The glass sheaths seem to remain intact after this step. This is also supported by the tip lateral views shown in the optical and SEM micrographs of Fig. 4, where it is

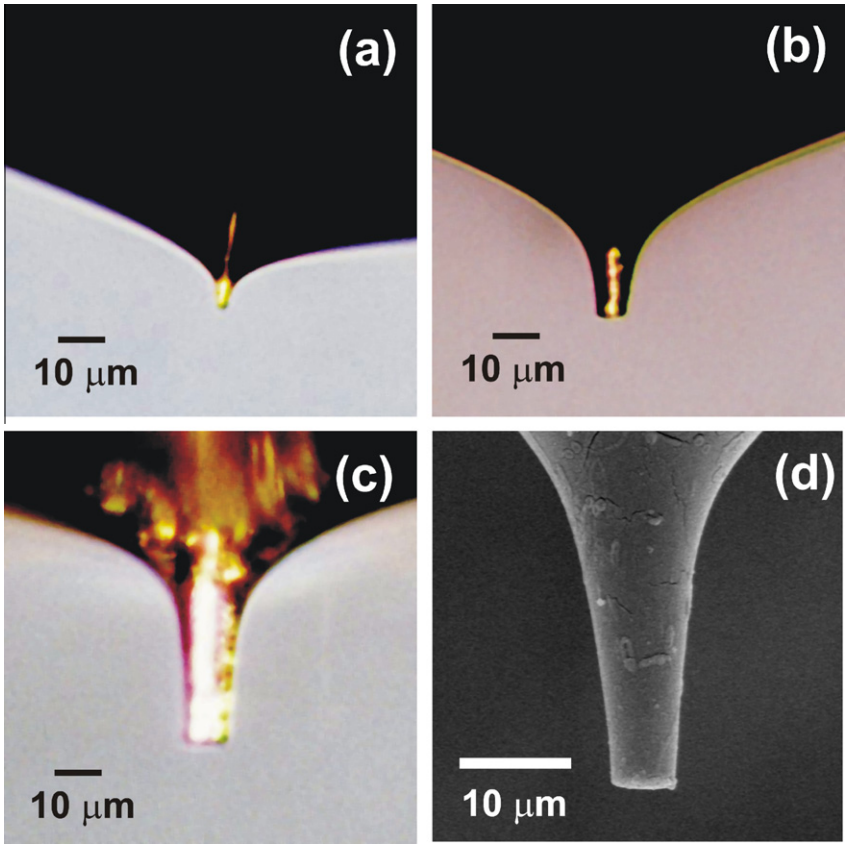


**Fig. 4.** Optical (a–c) and SEM (d) micrographs of polished-tip lateral views. In (d) the tip was coated with a sputtered gold layer.

Please cite this article in press as: H.L. Bonazza, J.L. Fernández, J. Electroanal. Chem. (2010), doi:10.1016/j.jelechem.2010.09.004

clearly observed that very flat cuts of the tip apex can be obtained by the described polishing method. Very low $R_g$ values (<2) can be roughly estimated for all Type-B tips as that shown in Fig. 3b. Even though the microelectrode radii could also be roughly estimated from the optical micrographs, these values could be misleading due to the difficulties for a precise detection of the Pt-glass boundaries.

Cyclic voltammetry of the tips before and after acrylic removal can provide evidences about the tip integrity, the quality of the disk, and of some tip features. In principle, the constancy of the voltammogram features upon taking the acrylic away should indicate that no uncoated Pt remained underneath the polished surface. However, we found that the limiting currents of the clean tips were always larger than those of the embedded tips, as it is shown for example in the voltammograms in Fig. 5. In some cases the limiting currents increased as much as 1.3 times. As will be shown below, these tips performed very well for SECM approach curves. Thus, these increases are likely caused by an effect of the extension of the insulating surface (or the $R_g$) [26], which goes from essentially infinite when the tip is embedded, to $R_g$ values smaller than 10 when the tip is clean.

### 3.2.1. Type-A tips

In the case of Type-A tips, the final disk size is determined by the accuracy for detecting the instant at which the polishing reaches the sealed-Pt apex. The exposition of the disk can be detected by fluctuations of the resistance between the Pt cone and an electrical contact immersed into the polishing slurry [24]. Before exposition the resistance should be out of scale even for a high-impedance ohmmeter. As soon as a disk with a few nanometers is free of glass this value decreases to the order of the GΩ [24], and quickly goes down to the MΩ upon increasing the disk size just a few more nanometers. We found that by using an ohmmeter able to measure up to 0.2 GΩ it is feasible to consistently detect exposition of disks with radii in the order of several hundreds of nanometers. It is possible that by using a high-impedance ohmmeter able to detect changes in the GΩ, such as that constructed by White and co-workers [24], even smaller disks could be obtained. Thus, Type-A tips should be useful when small (nanometer-sized) probes are required.

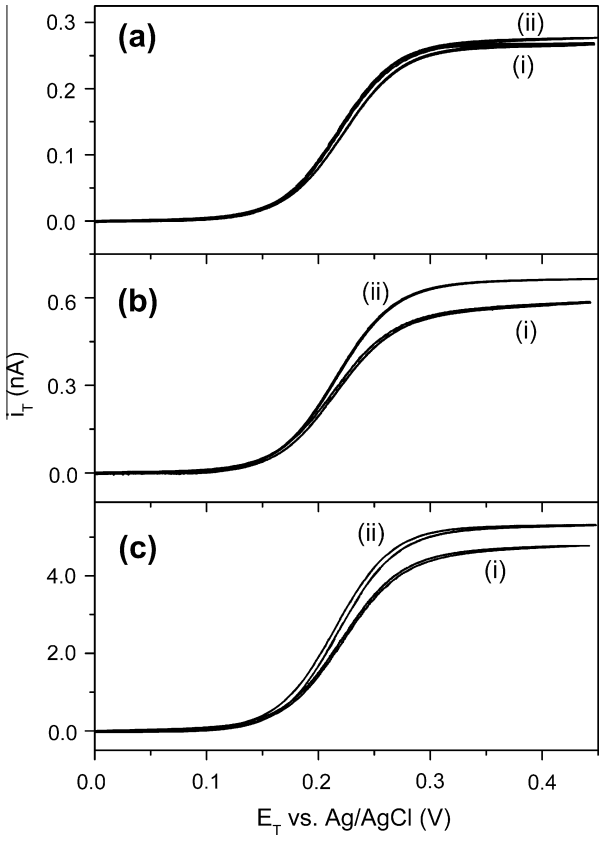


**Fig. 5.** Cyclic voltammograms in 3 mM FcMeOH–0.1 M $Na_2SO_4$ solution of Pt tips before (i) and after (ii) acrylic removal. Scan rate: 0.05 V $s^{-1}$.

### 3.2.2. Type-B tips

The most critical step for obtaining Type-A tips is the fabrication of a protruding Pt cone completely sealed in glass. By heating of the glass-coated sharpened Pt wire, melted glass flows and pulls the cone away. When the heating power is too high, the cone is exposed in just a few seconds and most of it is uncovered by glass. When the heating power is too low, the Pt wire bends at the glass surface. The result goes from one situation to the other in just a few degrees and a very fine control of the local temperature is required to get the projected cone completely shrouded. Besides, these conditions are strongly dependent on small changes of the cone sharpness and position into the capillary. For these reasons, the efficiency of this step is quite low (less than 30% of the tips are completely sealed). Even though different heating methods were tested, the best control was attained just by using a Bunsen flame under visual monitoring, as described in Section 2. Although the efficiency for obtaining fully coated cones was low with this method, in most of the cases where the Pt was exposed the size of the cone was quite small. These electrodes still can result in small disk-shaped tips after polishing the apex to a distance where the glass sheath is complete. However, it is difficult to know the exact time at which the height of the uncovered cone is completely removed and the Pt wire is totally surrounded by the glass sheath. For that reason, we implemented a method based on the resistance measurement between the Pt wire and an external conductive layer deposited onto the Pt cone and the glass capillary. A change in the resistance value from a few ohms to several MΩ indicated the transition of conductivity from a metal–metal contact to an ionic conductance through the wet polishing pad. Thus, this change signaled the point at which the smallest possible disk was separated from the Au coating by a continuous glass sheath. This can be observed for example in the optical micrographs of the upper views of supported tips shown in Figs. 2d-ii and 3b, where the Pt disk, the continuous glass sheath and the gold coating can be clearly detected. Fig. 3b also shows that after acrylic and gold removal the polished apex show no appreciable changes. In summary, Type-B tips are attractive when it is not required a very small microelectrode size, but low $R_g$ values are desired. It is obvious that the $R_g$ values could be larger if polishing is continued (as in the tip shown in Fig. 3c), in which case the metal coating for precise end-point detection is not necessary.

### 3.3. SECM performance of tips

The disk radii ($a$) could be roughly estimated from the values of the limiting currents at infinite distance ($i_{T,\infty}$) for FcMeOH oxidation and using Eq. (1) [26], where F is the Faraday constant, D and $C^*$ are the diffusion coefficient and bulk concentration of FcMeOH, respectively. The term $4FDC^*$ was calculated using a microelectrode disk with a known radius and near infinite $R_g$ value. However, as the tip current has a significant dependence with the $R_g$ value, for example according to Eq. (2) [27], the $a$ values of the tips were refined when fitting the approach curves.

$$i_{T,\infty} = 4FDC^* a\beta(R_g) \quad (1)$$

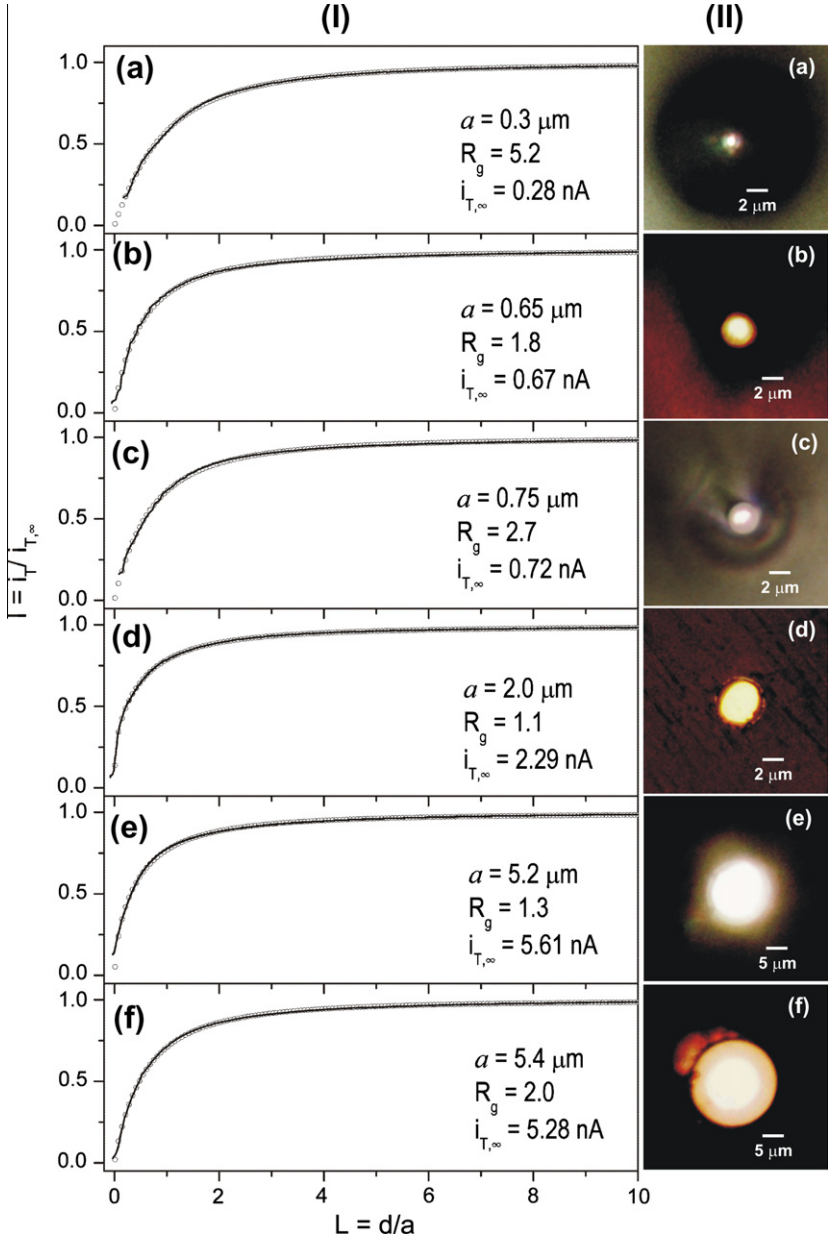


**Fig. 6.** (I) Negative-feedback approach curves of Pt tips measured over a Teflon surface (solid lines) and theoretical approach curves correlated using Eq. (3) (open symbols). The correlated $a$ and $R_g$ values, as well as the measured $i_{T,\infty}$ values, are indicated in each graph. Solution: 3 mM FcMeOH–0.1 M $Na_2SO_4$. $E_T$ = 0.45 V vs. Ag/AgCl. Approach rate: 0.5 μm $s^{-1}$. (II) Optical micrographs of the tips approached in (I).

$$\beta(R_g) = 1 + 0.639\left(1 - \frac{2}{\pi}\mathrm{ArcCos}\frac{1}{R_g}\right) - 0.168\left[1 - \left(\frac{2}{\pi}\mathrm{ArcCos}\frac{1}{R_g}\right)^2\right] \quad (2)$$

Negative-feedback (nf) approach curves were used to perform a full characterization of tip parameters, as these curves are very sensitive to the $R_g$ values [28]. Normalized nf approach curves ($I = i_T/i_{T,\infty}$ vs. $L = d/a$) that were measured over a polished Teflon surface are presented as solid lines in Fig. 6I, with the optical micrographs of the respective tips in Fig. 6II. In most cases, the tip current ($i_T$) values decreased to near 0.1–0.2 of the $i_{T,\infty}$ value. The experimental nf curves were correlated with Eqs. (1)–(3) [29,30] by a least square method, using $a$, the distance offset [31] and $R_g$ as adjustable parameters. The best-fitting curves are shown as open symbols in the respective graphs, and the resulting $a$ and $R_g$ values are reported. The fitting of these curves permitted to verify that tips with very low $R_g$ values (down to near 1.1) can be easily obtained by the described method.

$$I = \frac{\frac{2.08}{R_g^{0.358}}\left(L - \frac{0.145}{R_g}\right) + 1.585}{\frac{2.08}{R_g^{0.358}}\left(L + 0.0023R_g\right) + 1.57 + \frac{\ln(R_g)}{L} + \frac{2}{\pi R_g}\ln\left(1 + \frac{\pi R_g}{2L}\right)} \quad (3)$$

Positive-feedback (pf) approach curves were obtained over a Pt foil at open-circuit potential. Curves measured using tips with very low $R_g$ values (tips b, d and f in Fig. 6) are shown in Fig. 7. There always was at least a sixfold increase of $i_T$ respect to $i_{T,\infty}$ before the sheath border halted the approach. This indicates that these tips can be approached to tip-substrate distances in the order of one tenth of the microelectrode radius (or smaller) without much control of tip alignment and stage tilting. The pf curves simulated using Eq. (4) [27,30] and the tip parameters ($a$ and $R_g$) calculated

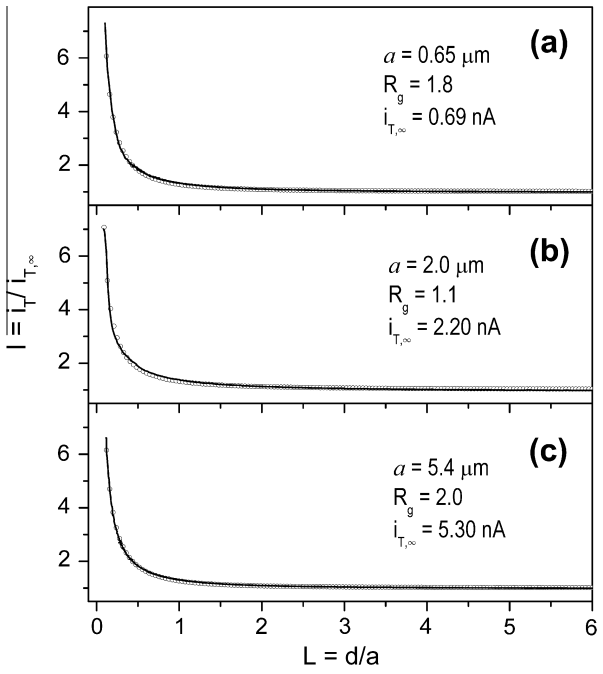


**Fig. 7.** Positive-feedback approach curves of Pt tips (b), (d) and (f) of Fig. 6 measured over a Pt foil (solid lines) and theoretical approach curves (open symbols) simulated using Eq. (5) with $a$ and $R_g$ values from Fig. 6. Solution: 3 mM FcMeOH–0.1 M $Na_2SO_4$. $E_T$ = 0.45 V vs. Ag/AgCl. Approach rate: 0.5 μm $s^{-1}$. The substrate was at open-circuit potential.

from the fitting of nf curves are included in Fig. 7 (open symbols). The theoretical and experimental curves overlap with reasonable accuracy, which is remarkable taking into account that the only adjustable parameter was the distance offset.

$$I = \alpha(R_g) + \frac{\pi}{4\beta(R_g)\mathrm{ArcTan}L} + \frac{2}{\pi}\left(1 - \alpha(R_g) - \frac{1}{2\beta(R_g)}\right)\mathrm{ArcTan}L \quad (4)$$

$$\alpha(R_g) = \ln 2 + \ln 2\left(1 - \frac{2}{\pi}\mathrm{ArcCos}\frac{1}{R_g}\right) - \ln 2\left[1 - \left(\frac{2}{\pi}\mathrm{ArcCos}\frac{1}{R_g}\right)^2\right] \quad (5)$$

From these results, it is verified that the described procedure for fabrication of microelectrodes leads to tips with low $R_g$ values that can function very well for SECM experiments in feedback mode.

## 4. Conclusions

A simple and efficient method for fabrication of SECM disk-shaped tips of any size and $R_g$ values was developed. The method can be used to prepare tips with conventional sizes (1–10 μm) and $R_g$ values (3–10). However, its main advantage is that it can be applied (keeping its simplicity and efficiency) for fabrication of tips with sub-micron radii and/or with very small $R_g$ values (typically smaller than 3). These tips can be approached to distances in the order of one tenth the microelectrode radius without much difficulty. A key feature of the method is that the polishing of the thermally sharpened tip is safely performed, which increases the success rate to more than 90%. The minimum tip size that is possible to obtain depends on the detection limit of the method used to identify the disk exposure instant. By using the conditions and instrumentation described in this work we were able to obtain tips with microelectrode radii as small as ~0.3 μm. The electrical method for detection of the optimum polishing endpoint may allow automating the polishing step.

## Acknowledgements

This work was supported by Agencia Nacional de Promoción Científica y Tecnológica (ANPCyT), Consejo Nacional de Investigaciones Científicas y Técnicas (CONICET) and Universidad Nacional del Litoral.

## References

[1] A.J. Bard, in: A.J. Bard, M.V. Mirkin (Eds.), Scanning Electrochemical Microscopy, Marcel Dekker, New York, 2001, p. 1 (Chapter 1).
[2] F.F. Fan, C. Demaille, in: A.J. Bard, M.V. Mirkin (Eds.), Scanning Electrochemical Microscopy, Marcel Dekker, New York, 2001, p. 75 (Chapter 3).
[3] F.F. Fan, J.L. Fernández, B. Liu, J. Mauzeroll, C.G. Zoski, in: C.G. Zoski (Ed.), Handbook of Electrochemistry, Elsevier, Amsterdam, 2007, p. 189 (Chapter 6).
[4] S. Amemiya, A.J. Bard, F.F. Fan, M.V. Mirkin, P.R. Unwin, Annu. Rev. Anal. Chem. 1 (2008) 95.
[5] C.G. Zoski, Electroanalysis 14 (2002) 1041.
[6] M.V. Mirkin, B.R. Horrocks, Anal. Chim. Acta 406 (2000) 119.
[7] Y. Shao, M.V. Mirkin, G. Fish, S. Kokotov, D. Palanker, A. Lewis, Anal. Chem. 69 (1997) 1627.
[8] B.B. Katemann, W. Schuhmann, Electroanalysis 14 (2002) 22.
[9] C. Yang, P. Sun, Anal. Chem. 81 (2009) 7496.
[10] J. Velmurugan, P. Sun, M.V. Mirkin, J. Phys. Chem. C 113 (2009) 459.
[11] P. Sun, M.V. Mirkin, Anal. Chem. 78 (2006) 6526.
[12] K.R.J. Lovelock, F.N. Cowling, A.W. Taylor, P. Licence, D.A. Walsh, J. Phys. Chem. B 114 (2010) 4442.
[13] B. Ballesteros Katemann, A. Schulte, W. Schuhmann, Electroanalysis 16 (2004) 60.
[14] F.O. Laforge, J. Velmurugan, Y. Wang, M.V. Mirkin, Anal. Chem. 81 (2009) 3143.
[15] D-H. Woo, H. Kang, S-M. Park, Anal. Chem. 75 (2003) 6732.
[16] J. Hu, K.B. Holt, J.S. Foord, Anal. Chem. 81 (2009) 5663.
[17] C. Lee, C.J. Miller, A.J. Bard, Anal. Chem. 63 (1991) 78.
[18] R.M. Penner, M.J. Heben, N.S. Lewis, Anal. Chem. 61 (1989) 1630.
[19] C.J. Slevin, N.J. Gray, J.V. Macpherson, M.A. Webb, P.R. Unwin, Electrochem. Commun. 1 (1999) 282.
[20] P. Sun, Z. Zhang, J. Guo, Y. Shao, Anal. Chem. 73 (2001) 5346.
[21] C.G. Zoski, B. Liu, A.J. Bard, Anal. Chem. 76 (2004) 3646.
[22] O. Sklyar, T.H. Treutler, N. Vlachopoulos, G. Wittstock, Surf. Sci. 597 (2005) 181.
[23] A.G. Güell, I. Díez-Pérez, P. Gorostiza, F. Sanz, Anal. Chem. 76 (2004) 5218.
[24] B. Zhang, J. Galusha, P.G. Shiozawa, G. Wang, A.J. Bergren, R.M. Jones, R.J. White, E.N. Ervin, C.C. Cauley, H.S. White, Anal. Chem. 79 (2007) 4778.
[25] Y. Li, D. Bergman, B. Zhang, Anal. Chem. 81 (2009) 5496.
[26] Y. Fang, J. Leddy, Anal. Chem. 67 (1995) 1259.
[27] C. Lefrou, J. Electroanal. Chem. 592 (2006) 103.
[28] J.L. Amphlett, G. Denuault, J. Phys. Chem. B 102 (1998) 9946.
[29] R. Cornut, C. Lefrou, J. Electroanal. Chem. 608 (2007) 59.
[30] C. Lefrou, R. Cornut, ChemPhysChem 11 (2010) 547.
[31] F.F. Fan, J.L. Fernández, B. Liu, J. Mauzeroll, in: C.G. Zoski (Ed.), Handbook of Electrochemistry, Elsevier, Amsterdam, 2007, p. 471 (Chapter 12).